Science and Technology Indonesia
e-ISSN:2580-4391 p-ISSN:2580-4405
Vol. 11, No. 3, July 2026

Research Paper

Land Cover Classification Using LAPAN-A3 and Sentinel-2 Imagery in Google Earth Engine: A Machine Learning-Based Comparative Analysis

Danang Budi Susetyo[1,2], Dewayany Sutrisno[3], Atriyon Julzarika[4], Agus Herawan[5*], Patria Rachman Hakim[5], Ahmad Fauzi[5]

[1]*Department of Geomatic Engineering. Yildiz Technical University, Istanbul, 34220, Türkiye*
[2]*National Research and Innovation Agency (BRIN), Jakarta, 10340, Indonesia*
[3]*Research Center for Climate and Atmosphere. National Research and Innovation Agency (BRIN), Bandung, West Java, 40135, Indonesia*
[4]*Research Center for Limnology and Water Resources. National Research and Innovation Agency (BRIN), Bogor, West Java, 16911, Indonesia*
[5]*Research Center for Satellite Technology. National Research and Innovation Agency (BRIN), Bogor, West Java, 16310, Indonesia*
*__Corresponding author__: agus112@brin.go.id

Abstract
Open-source satellite imagery such as Sentinel-2 has been widely proven reliable for various geospatial applications. However, achieving geospatial independence remains crucial for any country to reduce reliance on foreign data sources and strengthen national sovereignty in Earth observation capabilities. In this context, Indonesia initiated a microsatellite development program in 2007, which has now reached its third generation with LAPAN-A3. Despite these efforts, LAPAN-A3 is still considered an experimental satellite, and further evaluation is required before it can be fully adopted for operational applications. This study evaluates the performance of LAPAN-A3 imagery for land cover mapping using machine learning approaches and compares its performance with the well-established global dataset Sentinel-2. Two widely used classifiers, Random Forest (RF) and Support Vector Machine (SVM), were implemented within the Google Earth Engine (GEE) platform and tested using different combinations of spectral features. The results show consistent improvements in classification performance when additional spectral features are incorporated for both LAPAN-A3 and Sentinel-2 datasets. In all feature configurations, RF outperforms SVM, achieving higher Overall Accuracy (OA) and Kappa coefficients. Although Sentinel-2 generally yields slightly better results, LAPAN-A3 demonstrates promising performance despite its experimental nature. These findings highlight the potential of LAPAN-A3 as a national remote sensing asset that can contribute to Indonesia's long-term goal of achieving geospatial independence and strengthening domestic Earth observation capabilities.

Keywords
LAPAN-A3, Sentinel-2, Land Cover Classification, Machine Learning, Google Earth Engine (GEE)

Received: 6 April 2026, Accepted: 13 June 2026
https://doi.org/10.26554/sti.2026.11.3.1164-1175

1. INTRODUCTION

The advancement of remote sensing technology has significantly improved both data accessibility and processing capabilities. Open-source satellite imagery, such as Sentinel-2, has been proven reliable for various applications, including the identification of small land cover features such as tree cover (Eskandari et al., 2020; Ottosen et al., 2020) and human settlements (Corbane et al., 2021). However, achieving geospatial independence remains crucial for any country to reduce reliance on foreign products and technologies and to strengthen national sovereignty. Therefore, in 2007, the Indonesian National Institute of Aeronautics and Space (LAPAN), which is now integrated into the National Research and Innovation Agency (BRIN), initiated the development of a microsatellite program, beginning with LAPAN-A1/LAPAN-TUBSAT. The third generation of this program, LAPAN-A3/LAPAN-IPB, was successfully launched in 2016. This initiative marked an important step toward strengthening Indonesia's capabilities in space-based Earth observation.

However, LAPAN-A3 is still an experimental satellite, and further research is required before it can be considered for operational use. Moreover, microsatellites commonly have limitations in the spatial and spectral resolution of their optical sensors (Kurihara et al., 2020, 2018), meaning that their application, such as for land cover mapping, still needs to be further investigated. This limitation becomes more pronounced in fragmented tropical landscapes, where land cover patterns are highly heterogeneous and characterized by small and mixed land parcels. In such environments, medium-resolution imagery often struggles to capture fine-scale spatial variability. In

this context, a comparison with an established satellite, such as Sentinel-2, is necessary to assess the potential of the national satellite in reducing dependence on global satellite systems, which is the focus of this study.

Equipped with multiple payloads, including a multispectral push-broom imager, a digital matrix camera, and a video camera (Zylshal et al., 2017), the satellite supports a wide range of applications. Therefore, various studies had been carried out to evaluate its potential in remote sensing applications. These include DSM (Digital Surface Model) generation, the identification of geo-biophysical parameters (Julzarika, 2017), and monitoring of built-up areas, forests, water bodies, and agricultural lands (Khamsah et al., 2019; Setiawan et al., 2018). For land cover mapping, several studies have been conducted using LAPAN-A3 imagery, producing varied results with reported accuracies ranging from approximately 50% to 90% (Herawan et al., 2021; Nugroho et al., 2018; Zylshal et al., 2018). These findings emphasize the importance of LAPAN-A3 as a national satellite asset for remote sensing applications, particularly in land cover classification.

The advancement of GeoAI (Geospatial Artificial Intelligence), including the application of machine learning and deep learning to remote sensing data, has made land cover mapping research using LAPAN-A3 imagery increasingly important and relevant. Therefore, this study aims to optimize a well-established machine learning algorithm, namely Random Forest (RF) and Support Vector Machine (SVM), for land cover classification using LAPAN-A3 imagery. These algorithms are chosen for their many advantages, most notably their ability to achieve high classification accuracy (Avci et al., 2023; Thanh Noi and Kappas, 2017). Moreover, among decision tree–based algorithms, RF often achieves superior performance compared to others, although it is not the most computationally efficient (Shofiana et al., 2025). Therefore, comparing these two models remains highly relevant in advancing research on land cover classification and related applications.

Additionally, although GeoAI technologies continue to advance, both RF and SVM techniques remain widely used in remote sensing data classification in recent studies due to their robustness and reliability. Although RF is often recognized for its advantages, such as its ability to handle high-dimensional data and its robustness against overfitting (Belgiu and Drăguţ, 2016), as well as its efficiency in processing large input datasets (Adugna et al., 2022), several studies have shown that SVM can, in some cases, outperform RF (Erdanaev et al., 2022; Thanh Noi and Kappas, 2017; Zhang et al., 2023). On the other hand, tree-based methods tend to be sensitive to minor variations or noise in the training data, which can lead to instability (Resti et al., 2023).

This study investigates the performance of LAPAN-A3 imagery for land cover mapping using a machine learning approach, while also comparing its performance with a well-established global satellite dataset, Sentinel-2. The primary focus of this research lies in the utilization and evaluation of national satellite data rather than methodological development, so a well-established machine learning algorithms, RF and SVM, is employed. Through this approach, the study aims to provide a comprehensive assessment of the potential of LAPAN-A3 imagery for land cover classification and to highlight its viability as an alternative data source for large-scale geospatial applications, particularly in regions where national data availability plays a crucial role.

2. EXPERIMENTAL SECTION

2.1 Study Area

The study area is located in the southern part of Java Island, Indonesia, covering approximately 1,624 km^2 (Figure 1). The region is predominantly agricultural, with cropland as the main land cover type, alongside other categories such as built-up areas, natural vegetation, and water bodies. The selection of this area is based on two main considerations: (1) the availability of satellite imagery from both LAPAN-A3 and Sentinel-2 covering the same geographic extent, and (2) the presence of diverse and representative land cover classes suitable for classification assessment. In addition, the dominance of agricultural landscapes makes this region particularly relevant for evaluating the capability of medium-resolution satellite imagery in capturing detailed land cover patterns in tropical environments.

Climatically, the area is characterized by a tropical climate with distinct wet and dry seasons, which strongly influence vegetation dynamics and spectral responses across different land cover types. Seasonal variations in rainfall and vegetation phenology may affect the separability between classes such as cropland and natural vegetation. Topographically, the region is predominantly lowland, as it is located in a coastal area. These climatic and topographic conditions are important considerations, as they can influence spectral variability and, consequently, the performance of land cover classification models.

2.2 Data

Two satellite images covering the same study area, namely LAPAN-A3 and Sentinel-2, were acquired for analysis. The LAPAN-A3 imagery consists of four spectral bands (blue, green, red, and near-infrared/NIR), with a spatial resolution of 15 meters and a 16-bit radiometric resolution. The satellite has a revisit cycle of approximately 21 days. The image used in this study was acquired on May 3, 2021, in Level-1B format (radiometrically calibrated), with acquisition times ranging from 01:17:50 to 01:18:38 UTC.

The Sentinel-2 imagery was obtained through the Google Earth Engine (GEE) platform using the Surface Reflectance (SR) product. To ensure high-quality observations, images acquired during the year 2021 (to match the acquisition period of the LAPAN-A3 imagery) were selected and filtered based on a cloud cover threshold of less than 10%. A cloud and shadow masking procedure was applied using the Scene Classification Layer (SCL), where pixels corresponding to cloud, cirrus, cloud shadow, and snow were removed. The remaining observations were then composited using a median reducer to generate a cloud-free and temporally robust representation of the study

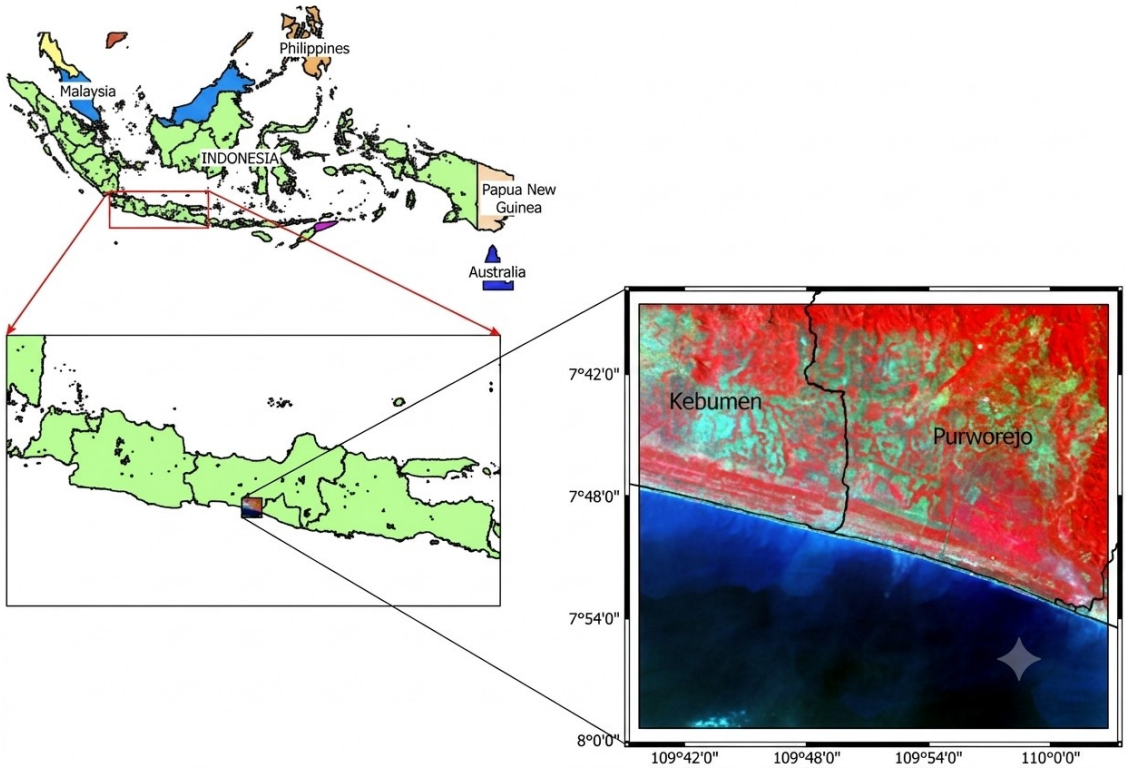

Figure 1. Location of the Study Area in Southern Java, Indonesia. The Right Panel Shows the Corresponding LAPAN-A3 Satellite Image

Table 1. Spectral Range Comparison Between LAPAN-A3 and Sentinel-2A Sensors (Modified From Zylshal et al. (2017))

Band	Sensor	Spectral Range (μm)	Spectral Bandwidth (nm)
Red	LAPAN-A3	0.63 – 0.70	70
	Sentinel-2A	0.698 – 0.713	15
Green	LAPAN-A3	0.51 – 0.58	70
	Sentinel-2A	0.650 – 0.680	30
Blue	LAPAN-A3	0.41 – 0.49	80
	Sentinel-2A	0.543 – 0.578	35
NIR	LAPAN-A3	0.77 – 0.99	220
	Sentinel-2A	0.855 – 0.875	20

area. With its high spatial resolution, frequent revisit time, and strong performance in land cover and vegetation analysis applications (Phiri et al., 2020), Sentinel-2 is widely recognized as a reliable reference dataset in Earth observation studies. A visual comparison between LAPAN-A3 and Sentinel-2 imagery is presented in Figure 2.

Table 1 presents the differences in spectral ranges between LAPAN-A3 and Sentinel-2A imagery, based on the information provided by Zylshal et al. (2017). Although the dataset used in this study is a combination of Sentinel-2A and Sentinel-2B, both satellites share highly similar sensor specifications and spectral characteristics. Therefore, Sentinel-2A is used as a representative reference for this comparison, given the strong similarity between Sentinel-2A and Sentinel-2B in terms of spectral response and reflectance behavior.

Then, as a comparison, Figure 3 illustrates the distribution of normalized pixel values for both Sentinel-2 and LAPAN-A3 imagery. Overall, the two datasets exhibit highly similar histogram patterns. For instance, the red, green, and blue bands are generally left-skewed, indicating a higher frequency of lower reflectance values, whereas the NIR band shows a slight shift toward higher values. However, Sentinel-2 demonstrates higher maximum pixel values compared to LAPAN-A3, while LAPAN-A3 tends to span a broader range of values. This suggests that although both datasets share comparable spectral distribution characteristics, differences in dynamic range and radiometric response may exist between the sensors.

LAPAN-A3 imagery has been radiometrically processed

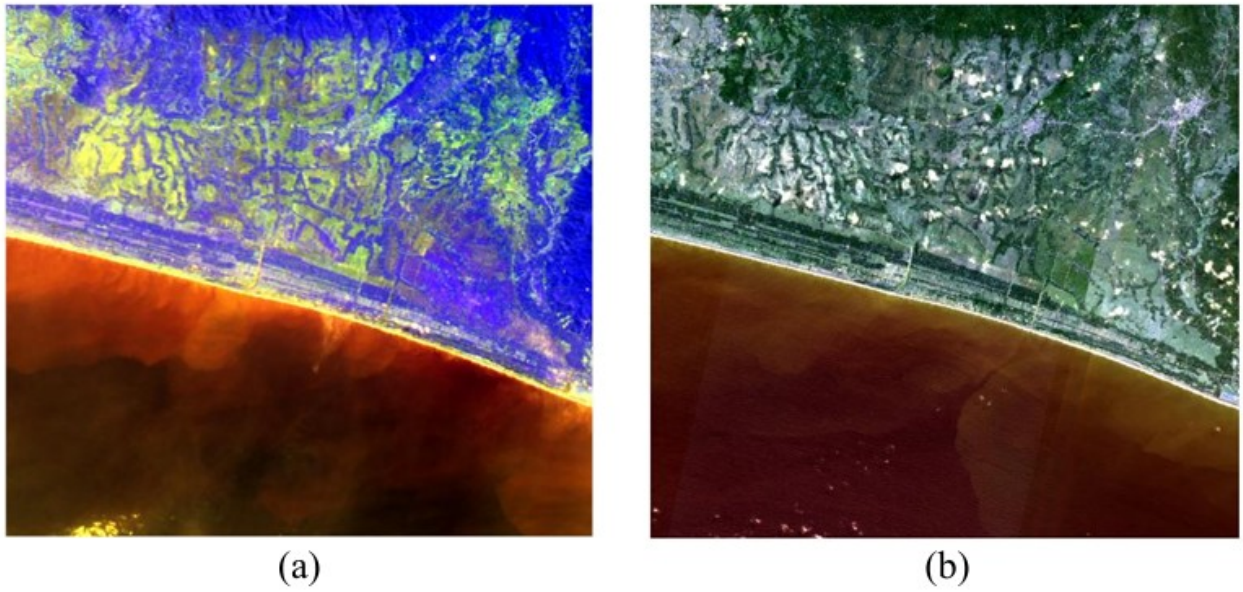

Figure 2. Visual Comparison of (a) LAPAN-A3 and (b) Sentinel-2 Imagery

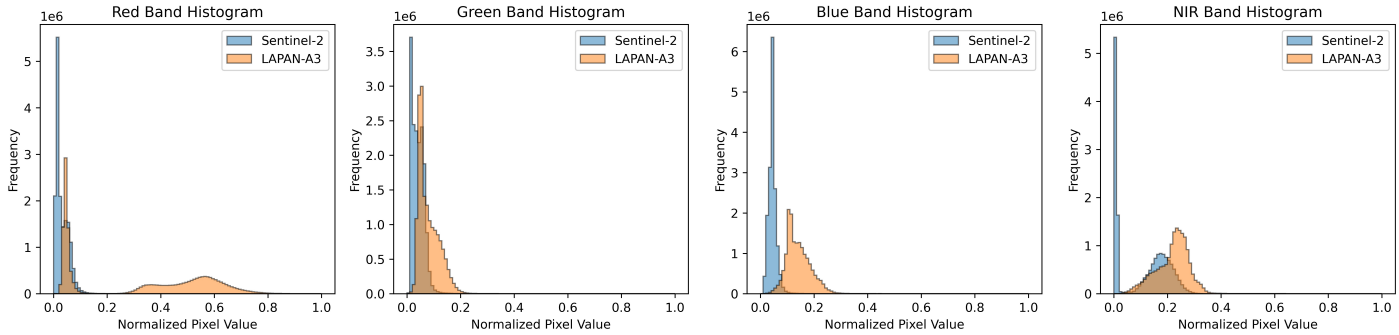

Figure 3. Normalized Pixel Value Histograms of Sentinel-2 and LAPAN-A3 Images Across Red, Green, Blue, and NIR Bands

by using pre-launch data calibration to correct vignetting distortion, as well as determination of top of atmosphere (ToA) radiance. However, atmospheric correction is only conducted case by case for imagery with significant haze and/or cloud cover. The imagery used in this research can be considered free of haze and/or cloud, therefore no additional processing needed more than standard systematic radiometric correction (Hakim et al., 2019). LAPAN-A3 preprocessing workflow show that in Figure 4.

2.3 Methods

The research flow diagram of this study is shown in Figure 5. This study employs Random Forest (RF) and Support Vector Machine (SVM) classifiers implemented within the Google Earth Engine (GEE) platform. The training dataset consists of labeled sample points representing four land cover classes: built-up, vegetation, cropland, and water. These four classes were selected because they represent the dominant land cover types in the study area and are most relevant to the objectives of this study. The classification scheme was simplified to ensure spectral separability and to reduce ambiguity due to the medium spatial resolution of the datasets used. Each class is represented by 400 sample points, resulting in a balanced and uniformly distributed training set across all categories. The same set of training samples is applied consistently to both image datasets to ensure a fair and comparable evaluation framework between LAPAN-A3 and Sentinel-2 data.

Sample point selection was conducted by ensuring consistent land cover interpretation between Sentinel-2 and LAPAN-A3 imagery. A manual visual interpretation approach was applied, where land cover classes were identified by visually examining both datasets to ensure labeling consistency across sensors. This cross-sensor interpretation helped reduce potential misclassification arising from differences in spatial resolution and spectral characteristics. Subsequently, sample points were distributed in a spatially balanced manner across the entire study area for all land cover classes. Within each class, sampling locations were deliberately placed to capture a wide range of spatial

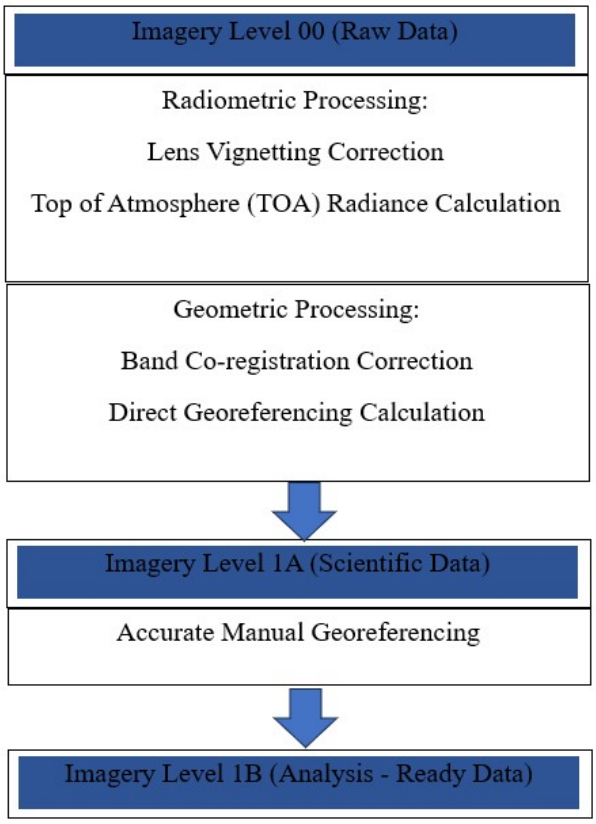

Figure 4. LAPAN-A3 Preprocessing Workflow

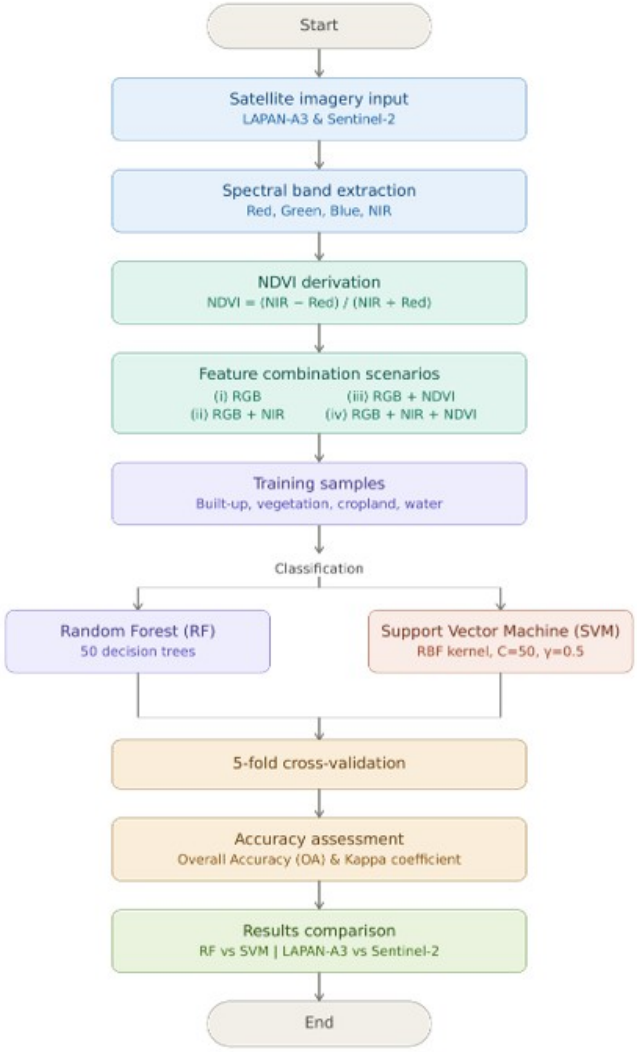

Figure 5. Flowchart Illustrating the Research Methodology of This Study

conditions, ensuring that different landscape patterns and heterogeneity within the study area were adequately represented. This strategy was adopted to enhance the representativeness of the training data and to minimize potential spatial bias in the classification process.

Multiple feature combinations were systematically evaluated for both LAPAN-A3 and Sentinel-2 imagery to examine the influence of spectral information and derived indices on classification performance. A consistent set of spectral bands: red, green, blue, and near-infrared (*NIR*), was used across both datasets, and these bands were arranged into different configurations to assess how variations in feature composition affect model accuracy. In addition to the original spectral bands, the Normalized Difference Vegetation Index (*NDVI*) was derived from the NIR and red bands (Equation 1) and incorporated as an additional feature to capture vegetation-related variability more effectively. *NDVI* is defined as the normalized ratio between NIR and red reflectance values:

$$NDVI = \frac{NIR - Red}{NIR + Red} \quad (1)$$

where *NIR* and Red denote the reflectance values of the near-infrared and red spectral bands, respectively. Based on these inputs, four feature scenarios were constructed: (i) RGB (visible bands only), (ii) RGB + NIR, (iii) RGB + NDVI, and (iv) RGB + NIR + NDVI. These feature sets were designed to systematically evaluate the contribution of near-infrared information and vegetation index features in improving class separability across different land cover types.

In this study, the RF model was configured with 50 decision trees. This number was selected to achieve a balance between computational efficiency and classification stability. While several studies have reported that optimal performance can be achieved using a relatively large number of trees (Chen et al., 2023; Mohammadpour et al., 2022; Plakman et al., 2020), other studies have also demonstrated that satisfactory results can be obtained with a lower number of trees (Amini et al., 2022). Other studies have also demonstrated decision tree in water quality classification. As a result, RF finished at an impressive test result with 98% of accuracy (Shofiana et al.,

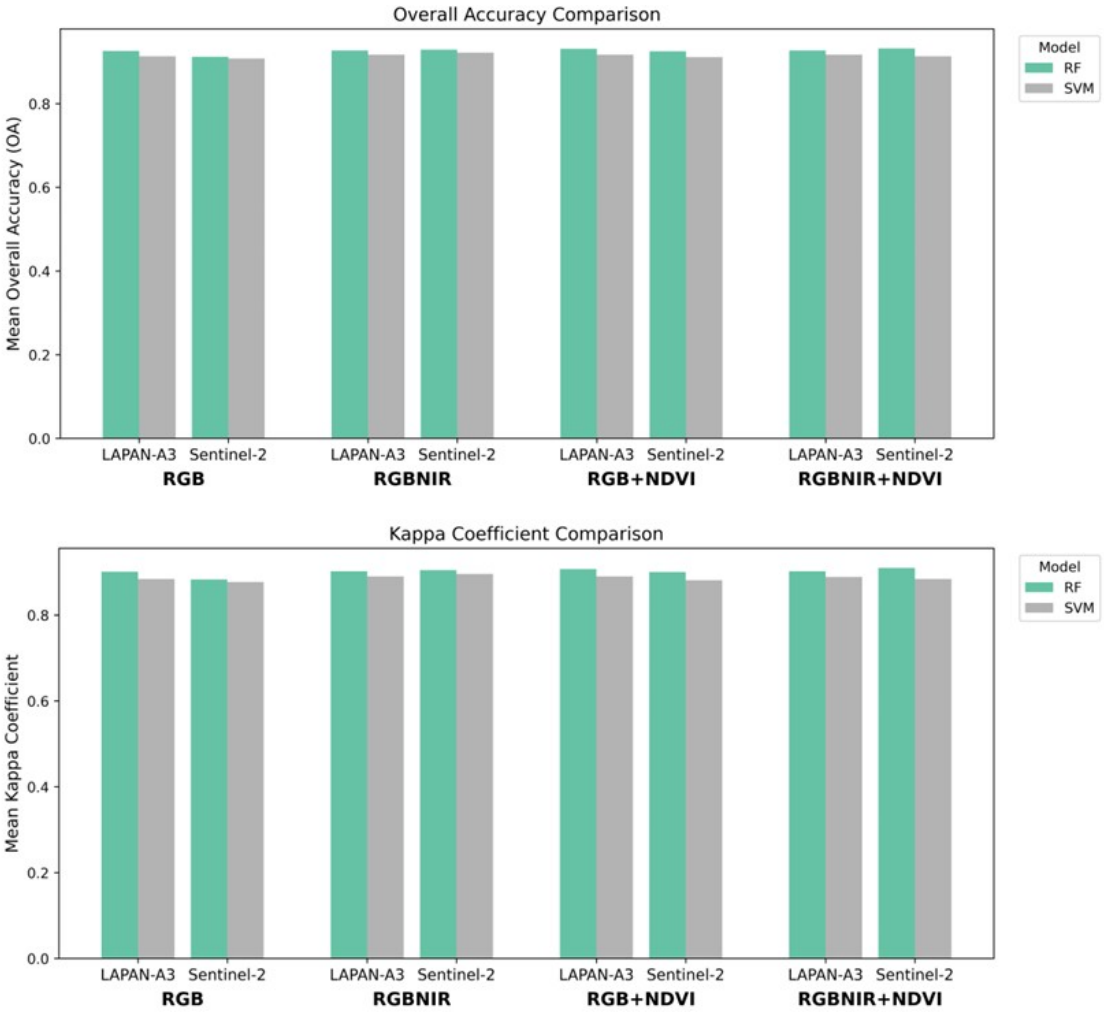

Figure 6. Comparison of Mean Overall Accuracy (OA) (Top) and Mean Kappa Coefficient (Bottom) Across Different Feature Combinations and Classifiers for LAPAN-A3 and Sentinel-2

2025). In general, a moderate number of trees is sufficient to ensure stable ensemble convergence while reducing unnecessary computational cost, particularly in large-scale remote sensing applications with extensive spatial coverage.

On the other hand, the SVM classifier was implemented using a Radial Basis Function (RBF) kernel and configured with a cost parameter (C = 50) and a gamma value (γ = 0.5). These parameters were selected based on commonly adopted configurations in remote sensing studies and preliminary sensitivity checks. The RBF kernel was chosen due to its effectiveness in handling complex, non-linearly separable patterns that are typically present in multispectral remote sensing data. The cost parameter (C = 50) controls the trade-off between maximizing the margin and minimizing classification errors. Meanwhile, the gamma parameter (γ = 0.5) defines the influence of individual training samples on the decision boundary, enabling the model to capture spatial and spectral variability while maintaining generalization capability. Overall, this configuration provides a balanced setting between model flexibility and robustness across different feature combinations.

No systematic hyperparameter optimization was conducted in this study. Instead, a fixed-parameter setting was adopted to ensure consistency across all feature sets and to enable a fair comparison between LAPAN-A3 and Sentinel-2 datasets. This approach also helps isolate the effect of input feature combinations on classification performance without introducing additional variability from parameter tuning. Consequently, the reported results reflect the inherent discriminatory power of the datasets rather than model-specific optimization.

To ensure a robust and reliable assessment, a 5-fold cross-validation strategy was adopted. The dataset was randomly partitioned into five approximately equal subsets (folds). In each iteration, one fold was used as the testing set, while the remaining four folds were used for model training. Classification performance was evaluated using two standard metrics: Overall Accuracy (OA) and the Kappa coefficient, with the correspond-

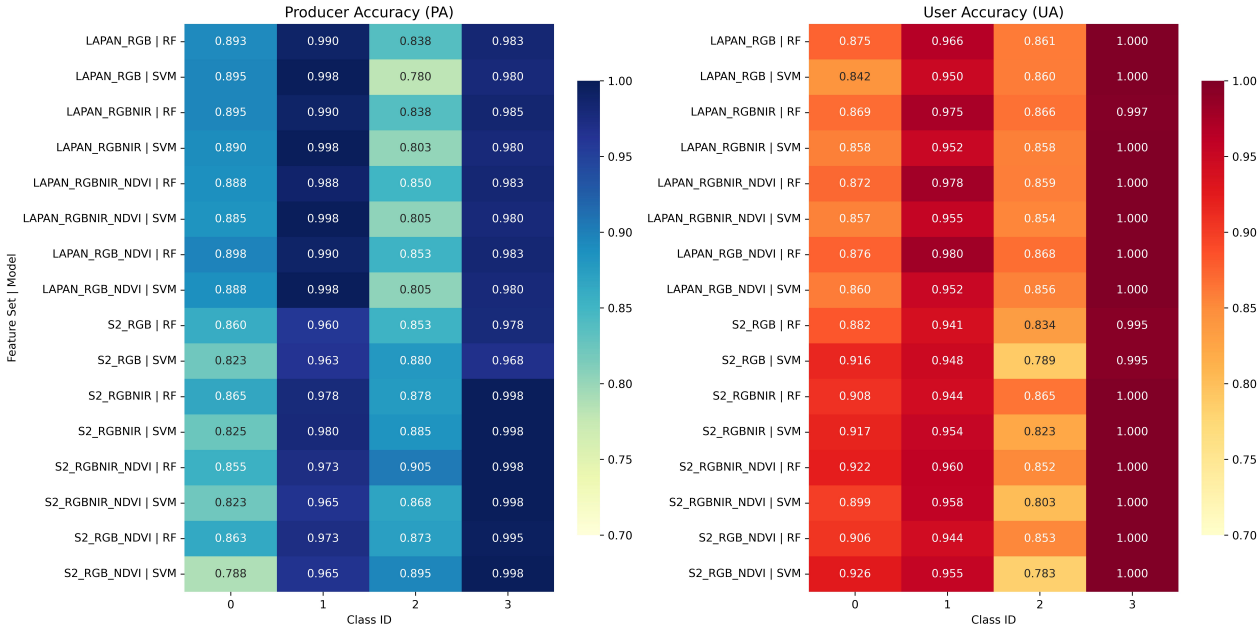

Figure 7. Heatmap Visualization of Producer's Accuracy (PA) and User's Accuracy (UA) Across Different Feature Sets, Classifiers, and Land Cover Classes

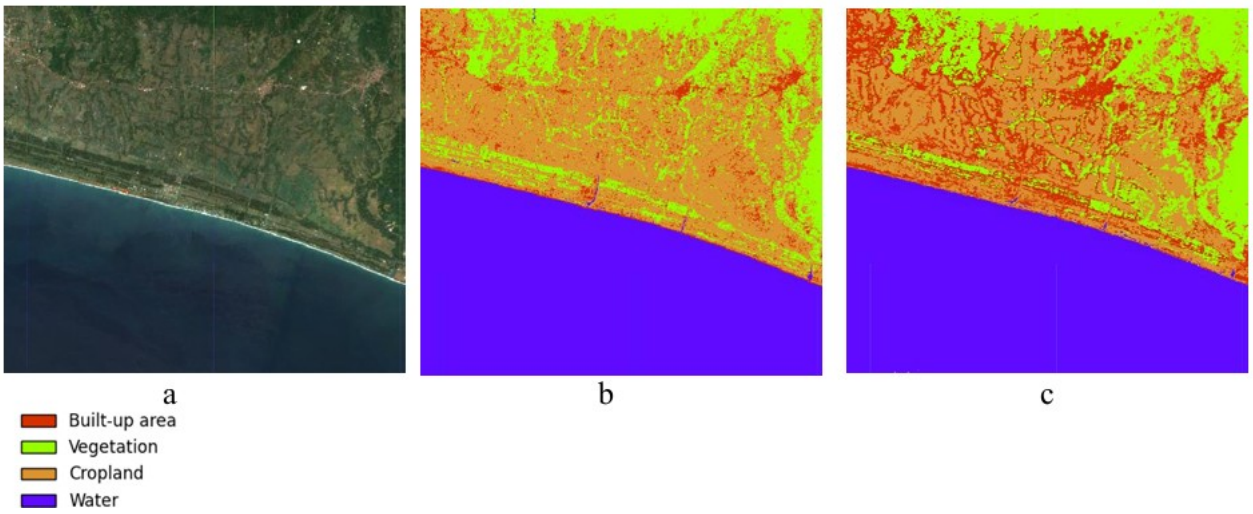

Figure 8. Comparison Between Sentinel-2 and LAPAN-A3 Based Land Cover Classification Results Using Random Forest (RF) and Combined RGB, NIR, and NDVI Features. (a) Sentinel-2 RGB Composite Image, (b) Classification Result from Sentinel-2, and (c) Classification Result from LAPAN-A3

ing equation presented in Equations 2 and 3. The evaluation metrics were computed for each fold, and the final reported results represent the mean values across all folds for each feature combination and classifier. This averaging approach provides a more stable and reliable estimate of model performance, reducing the influence of random sampling variability and enabling a fair comparison between models.

$$\text{OA} = \frac{\text{Number of points that classified correctly}}{\text{Total sample points}} \tag{2}$$

$$\kappa = \frac{p_o - p_e}{1 - p_e} \tag{3}$$

where p_o represents the observed proportion of agreement between the classification results and the reference data, and

Table 2. Comparison of Mean Overall Accuracy (OA) and Kappa Coefficient for LAPAN-A3 and Sentinel-2 Using Different Feature Combinations and Classification Models

Image	Feature Set	Model	OA_mean	OA_std	Kappa_mean	Kappa_std
LAPAN-A3	RGB	RF	0.926	0.005	0.901	0.007
		SVM	0.913	0.009	0.884	0.012
	RGB+NIR	RF	0.927	0.008	0.902	0.010
		SVM	0.917	0.010	0.890	0.014
	RGB+NDVI	RF	0.931	0.009	0.907	0.012
		SVM	0.917	0.010	0.890	0.014
	RGB+NIR+NDVI	RF	0.927	0.005	0.902	0.007
		SVM	0.917	0.010	0.889	0.013
Sentinel-2	RGB	RF	0.912	0.011	0.883	0.014
		SVM	0.908	0.016	0.877	0.022
	RGB+NIR	RF	0.929	0.014	0.905	0.019
		SVM	0.922	0.012	0.896	0.016
	RGB+NDVI	RF	0.925	0.014	0.900	0.019
		SVM	0.911	0.015	0.881	0.019
	RGB+NIR+NDVI	RF	0.932	0.015	0.910	0.020
		SVM	0.913	0.009	0.884	0.012

Table 3. Contingency Table of Paired RF and SVM Classification Results Used for the McNemar Test

	SVM Correct	SVM Wrong	Total
RF Correct	11459	397	11856
RF Wrong	252	692	944
Total	11711	1089	12800

p_e denotes the expected probability of agreement occurring by chance.

3. RESULTS AND DISCUSSIONS

The classification results are presented in Table 2 and visualized as bar charts in Figure 6 for clearer comparison across feature combinations and classifiers. Overall, the results demonstrate consistent performance improvements with the inclusion of additional spectral features for both LAPAN-A3 and Sentinel-2. In general, RF consistently outperforms SVM across all feature combinations, not only in terms of higher mean Overall Accuracy (OA) and Kappa values, but also in terms of lower standard deviations, indicating greater stability across cross-validation folds.

For LAPAN-A3, the best performance is achieved using the RGB+NDVI feature set with RF (OA = 0.931 ± 0.009; Kappa = 0.907 ± 0.012), suggesting that vegetation-related indices significantly improve class separability. Meanwhile, Sentinel-2 exhibits stronger performance gains with the integration of both NIR and NDVI, where the highest accuracy is obtained from the RGB+NIR+NDVI combination using RF (OA = 0.932 ± 0.015; Kappa = 0.910 ± 0.020). Although Sentinel-2 slightly outperforms LAPAN-A3 at its optimal configuration, both sensors show comparable overall performance patterns. These results highlight the effectiveness of incorporating additional spectral information, as well as the robustness of RF for land cover classification tasks.

Subsequently, a class-wise accuracy assessment was conducted using Producer's Accuracy (PA) and User's Accuracy (UA) to evaluate the robustness of the classification results across different feature combinations and classifiers. Overall, the vegetation and water classes consistently achieved the highest accuracy values, with both PA and UA frequently exceeding 0.95 for both RF and SVM models. The vegetation class shows strong performance due to its dominance in the study area and its relatively distinct spectral characteristics, while the water class also yields high accuracy, largely because most reference samples are located in coastal and marine areas with clear spectral separation. In contrast, the urban and cropland classes exhibit comparatively lower accuracies. This can be attributed to the higher intra-class complexity, spectral similarity between these classes, and the presence of mixed pixels in heterogeneous transition zones, which collectively reduce classification performance. The PA and UA values are further visualized in Figure 7 using heatmaps for a clearer comparison across classes, feature sets, and classifiers.

To evaluate whether there is a statistically significant difference between the RF and SVM classifiers, McNemar's test was applied using paired predictions derived from the same test samples. The matched-pair results are summarized in Table 3. In this analysis, a contingency table was constructed based on the number of instances where RF correctly classified samples while SVM did not (b = 397), and vice versa (c = 252). The test assesses whether the disagreement between the two classifiers is symmetric, indicating comparable performance, or asymmetric, indicating a significant difference. The results show that RF correctly classified more samples that were misclassified

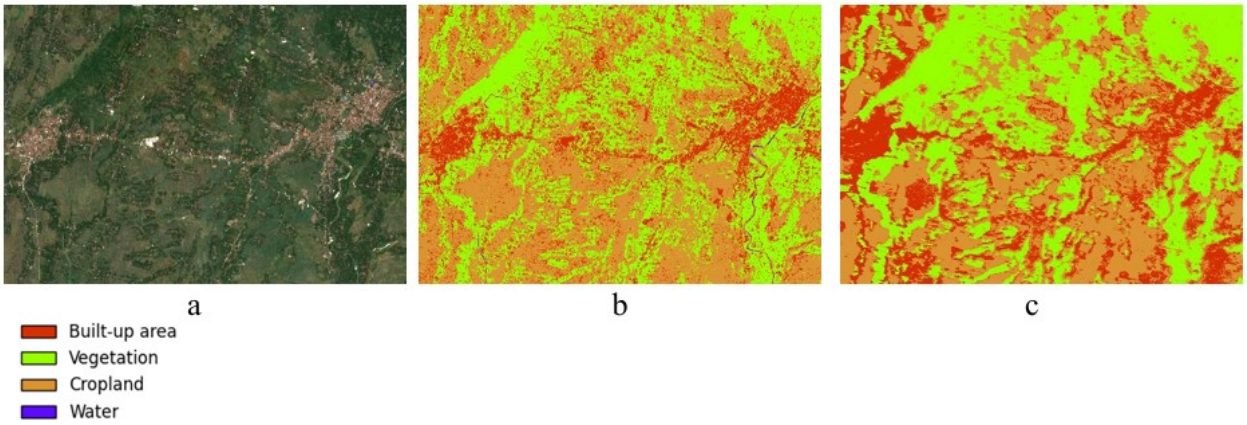

Figure 9. Comparison of Sentinel-2 and LAPAN-A3 Over a Residential Area Surrounded by Vegetation. (a) Sentinel-2 RGB Composite Image, (b) Classification Result from Sentinel-2, and (c) Classification Result from LAPAN-A3

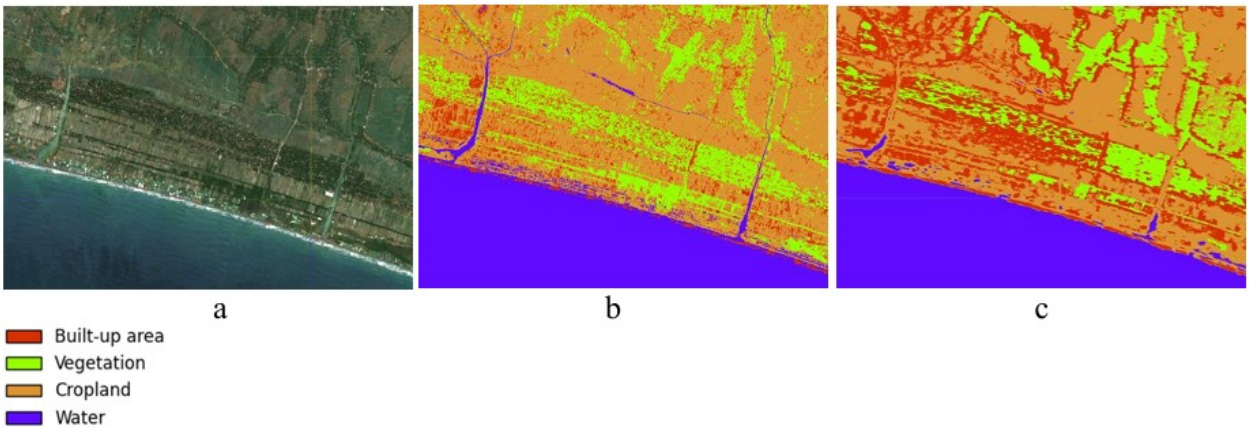

Figure 10. Comparison of Sentinel-2 and LAPAN-A3 in Coastal Area. (a) Sentinel-2 RGB Composite Image, (b) Classification Result from Sentinel-2, and (c) Classification Result from LAPAN-A3

by SVM compared to the opposite case. The McNemar test yielded a chi-square value of 31.951 with $p < 0.001$, indicating a statistically significant difference between the two classifiers. This result suggests that the RF classifier significantly outperforms the SVM classifier in terms of classification accuracy for the given dataset.

For the visual analysis, the classification results derived from the RGB+NIR+NDVI dataset using the RF algorithm were selected (Figure 8). Overall, Sentinel-2 produces visually more balanced and consistent classification results compared to LAPAN-A3. Land cover classes appear to be mapped in a more proportional manner, whereas LAPAN-A3 shows a tendency toward overestimation in certain classes, particularly the built-up class, which is frequently confused with cropland. This indicates potential spectral similarity or misclassification between these two classes in LAPAN-A3 data. However, LAPAN-A3 demonstrates reliable performance in vegetation class, where the spatial patterns are largely consistent with those derived from Sentinel-2. In addition, water bodies, particularly in coastal and marine areas, are classified with relatively good accuracy. This suggests that LAPAN-A3 has potential applicability for rapid coastal mapping and shoreline delineation.

Figure 9 presents the classification results of LAPAN-A3 and Sentinel-2 over a residential area surrounded by vegetation. Overall, both datasets exhibit a broadly similar spatial pattern in representing built-up and vegetated areas, indicating general consistency between the two sensors. However, a closer inspection reveals notable differences in spatial detail and classification smoothness. The LAPAN-A3 results tend to produce more spatially homogeneous and "smoothed" class regions, where vegetation and built-up areas appear as more continuous and consolidated patches. In contrast, Sentinel-2 results exhibit a higher level of spatial variability, with a more fragmented or "speckled" pattern, particularly along class boundaries. In addition, LAPAN-A3 shows greater difficulty in accurately delineating small residential structures embedded within cropland and dense vegetation. These small built-up features are often absorbed into the surrounding classes, leading to an overesti-

mation of vegetated areas and cropland, and a corresponding underrepresentation of fine-scale settlements.

The classification results in coastal areas are presented in Figure 10. Overall, LAPAN-A3 demonstrates relatively good performance in identifying water bodies in coastal and marine environments. This indicates that LAPAN-A3 has promising potential for rapid coastal mapping and basic shoreline delineation, where spectral contrast between land and water is generally strong. However, mixed pixels are likely to occur along coastlines and estuarine zones due to the transitional nature of land-water interfaces, which introduces uncertainty in shoreline delineation. Notable differences emerge when compared with Sentinel-2, especially in fluvial environments. Sentinel-2 is able to delineate river systems more accurately and consistently, capturing the finer geometric structure of river channels. In contrast, LAPAN-A3 struggles to represent river geometry in sufficient detail, often resulting in less well-defined classifications along narrow watercourses. This limitation suggests that while LAPAN-A3 is suitable for broader-scale water body extraction, its performance decreases in environments that require fine spatial resolution and precise linear feature representation, such as rivers and small tributaries.

The classification results obtained in this study can be interpreted in relation to the radiometric characteristics of the Sentinel-2 and LAPAN-A3 datasets. As shown in Figure 3, both sensors exhibit broadly similar histogram distributions across spectral bands, indicating that they capture comparable spectral information. This similarity helps explain why the overall classification performance between the two datasets is relatively close.

The classification results indicate that both LAPAN-A3 and Sentinel-2 datasets achieve consistently high performance across all feature combinations and classifiers. Overall, the obtained OA values range from approximately 0.908 to 0.932, while the Kappa coefficient ranges from 0.877 to 0.910. These results suggest that both datasets are highly capable of discriminating land cover classes in the study area, despite differences in spatial resolution and sensor characteristics. This finding is consistent with previous studies highlighting the applicability of LAPAN-A3 for land cover mapping and related remote sensing applications.

In general, Sentinel-2 shows slightly superior performance compared to LAPAN-A3, particularly when using enriched spectral feature sets. Across both sensors, the addition of spectral bands consistently improves classification performance compared to the baseline RGB configuration. The inclusion of NIR enhances the ability to separate vegetated and non-vegetated areas, while NDVI further strengthens the discrimination of vegetation-related classes. The highest accuracy is achieved by Sentinel-2 using the RGB+NIR+NDVI combination with RF algorithm. This indicates that higher spectral richness, especially the inclusion of NIR and NDVI, significantly enhances class separability, particularly for vegetation and built-up discrimination. LAPAN-A3 also demonstrates strong performance, with its best result obtained from the RGB+NDVI configuration, suggesting that vegetation-sensitive indices play a crucial role. It shows that the improvement is not strictly linear, indicating that the contribution of additional bands may depend on the interaction between spectral information and classifier sensitivity.

In terms of agreement measure, the Kappa coefficient follows a similar pattern to OA, confirming the robustness of the classification results. High Kappa values across all experiments indicate a strong agreement between predicted and reference classes beyond chance agreement. Sentinel-2 with RGB+NIR+NDVI and RF algorithm exhibits the highest Kappa value, reinforcing its reliability in producing consistent classification outputs. Meanwhile, LAPAN-A3 maintains comparable Kappa values, demonstrating that despite its limitations in spatial resolution, it still provides reliable classification performance when appropriate feature combinations are used.

Regarding the classification algorithms, RF consistently outperforms SVM across all scenarios, albeit with relatively small margins. This suggests that although SVM is known for its strong generalization capability, particularly in scenarios with limited training samples (Mountrakis et al., 2011; Sheykhmousa et al., 2020), ensemble-based methods such as RF are more effective in handling the variability and complexity of spectral feature spaces in this dataset. Overall, the results confirm that both sensor quality and feature engineering play a critical role in improving land cover classification accuracy, with Sentinel-2 providing a slight but consistent advantage when combined with richer spectral inputs.

Although the classification accuracies of Sentinel-2 and LAPAN-A3 are relatively close, Sentinel-2 generally provides more realistic and spatially consistent results compared to LAPAN-A3. This difference can be attributed to several factors. First, LAPAN-A3 tends to overestimate the built-up class, particularly in heterogeneous landscapes. It also struggles to accurately delineate small residential structures embedded within vegetation or cropland, a task that Sentinel-2 handles more effectively due to its more stable spectral response and higher radiometric consistency. Second, LAPAN-A3 shows limitations in representing river geometries, especially in narrow river segments, where classification results are often discontinuous or less well-defined. In contrast, Sentinel-2 is able to capture these linear water features with greater clarity and spatial coherence. Although Sentinel-2 demonstrates superior performance in medium-resolution land cover mapping applications, LAPAN-A3 still holds significant potential as a national remote sensing asset, as evidenced by its relatively high classification accuracy. It also plays an important role in supporting Indonesia's efforts toward technological independence in geospatial data acquisition and Earth observation systems.

4. CONCLUSIONS

This study investigates the application of LAPAN-A3 imagery for land cover classification and compares its performance with an established global satellite dataset, Sentinel-2. The experiments were conducted by evaluating two machine learning

algorithms, Random Forest (RF) and Support Vector Machine (SVM), using different spectral feature combinations, including RGB bands, Near-Infrared (NIR), and NDVI. The results indicate that Sentinel-2 slightly outperforms LAPAN-A3 in terms of classification accuracy. In addition, the RF algorithm consistently demonstrates better performance than SVM, particularly when additional spectral features are incorporated. Nevertheless, LAPAN-A3 still shows promising overall performance, although certain limitations remain, such as overestimation in specific land cover classes. These findings highlight the strong potential of LAPAN-A3 as a national remote sensing asset that can contribute to Indonesia's future geospatial independence. For future research, more contemporary approaches such as deep learning methods could be explored. Furthermore, data fusion strategies, for instance integrating LAPAN-A3 with Sentinel-2, may help improve classification accuracy. Time-series analysis is also recommended to assess the potential of LAPAN-A3 for land cover change detection and temporal monitoring. Comprehensive evaluation of LAPAN-A3 across different application domains can offer a deeper understanding of its capabilities and broader potential for operational use.

5. ACKNOWLEDGEMENT

The authors are grateful to Research Center for Satellite Technology, National Research and Innovation Agency of Indonesia (BRIN) for LAPAN-A3 data support.

REFERENCES

Adugna, T., W. Xu, and J. Fan (2022). Comparison of Random Forest and Support Vector Machine Classifiers for Regional Land Cover Mapping Using Coarse Resolution FY-3C Images. *Remote Sensing*, **14**(3); 574

Amini, S., M. Saber, H. Rabiei-Dastjerdi, and S. Homayouni (2022). Urban Land Use and Land Cover Change Analysis Using Random Forest Classification of Landsat Time Series. *Remote Sensing*, **14**(11); 2654

Avci, C., M. Budak, N. Yagmur, and F. B. Balcik (2023). Comparison Between Random Forest and Support Vector Machine Algorithms for LULC Classification. *International Journal of Engineering and Geosciences*, **8**(1); 1–10

Belgiu, M. and L. Drăguţ (2016). Random Forest in Remote Sensing: A Review of Applications and Future Directions. *ISPRS Journal of Photogrammetry and Remote Sensing*, **114**; 24–31

Chen, T.-H. K., B. Pandey, and K. C. Seto (2023). Detecting Subpixel Human Settlements in Mountains Using Deep Learning: A Case of the Hindu Kush Himalaya 1990-2020. *Remote Sensing of Environment*, **294**; 113625

Corbane, C., V. Syrris, F. Sabo, P. Politis, M. Melchiorri, M. Pesaresi, and T. Kemper (2021). Convolutional Neural Networks for Global Human Settlements Mapping from Sentinel-2 Satellite Imagery. *Neural Computing and Applications*, **33**; 6697–6720

Erdanaev, E., M. Kappas, and D. Wyss (2022). The Identification of Irrigated Crop Types Using Support Vector Machine, Random Forest and Maximum Likelihood Classification Methods with Sentinel-2 Data in 2018: Tashkent Province, Uzbekistan. *International Journal of Geoinformatics*, **18**(2); 37–53

Eskandari, S., M. Reza Jaafari, P. Oliva, O. Ghorbanzadeh, and T. Blaschke (2020). Mapping Land Cover and Tree Canopy Cover in Zagros Forests of Iran: Application of Sentinel-2, Google Earth, and Field Data. *Remote Sensing*, **12**(12); 1912

Hakim, P. R., A. H. Syafrudin, S. Salaswati, S. Utama, and W. Hasbi (2019). Development of Systematic Image Preprocessing of LAPAN-A3/IPB Multispectral Images. *International Journal of Advanced Studies Incomputer Science in Engineering*, **7**(10); 9–18

Herawan, A., A. Julzarika, P. R. Hakim, and E. A. Anggari (2021). Object-Based Land Cover Classification on LAPAN-A3 Satellite Imagery Using Tree Algorithm (Case Study: Rote Island). *International Journal on Advanced Science, Engineering and Information Technology*, **11**(6); 2254–2260

Julzarika, A. (2017). Utilization of LAPAN Satellite (TUBSAT, A2, and A3) in Supporting Indonesia's Potential as Maritime Center of the World. In *IOP Conference Series: Earth and Environmental Science*, volume 54. IOP Publishing, page 012097

Khamsah, N. M. N., S. Utama, R. H. Surayuda, and P. R. Hakim (2019). The Development of LAPAN-A3 Satellite Off-Nadir Imaging Mission. In *2019 IEEE International Conference on Aerospace Electronics and Remote Sensing Technology (ICARES)*. IEEE, pages 1–6

Kurihara, J., T. Kuwahara, S. Fujita, Y. Sato, K. Hanyu, M. Sakai, and W.-H. Ip (2020). A High Spatial Resolution Multispectral Sensor on the RISESAT Microsatellite. *Transactions of the Japan Society for Aeronautical and Space Sciences, Aerospace Technology Japan*, **18**(5); 186–191

Kurihara, J., Y. Takahashi, Y. Sakamoto, T. Kuwahara, and K. Yoshida (2018). HPT: A High Spatial Resolution Multispectral Sensor for Microsatellite Remote Sensing. *Sensors*, **18**(2); 1–11

Mohammadpour, P., D. X. Viegas, and C. Viegas (2022). Vegetation Mapping with Random Forest Using Sentinel 2 and GLCM Texture Feature-A Case Study for Lousã Region, Portugal. *Remote Sensing*, **14**(18); 4585

Mountrakis, G., J. Im, and C. Ogole (2011). Support Vector Machines in Remote Sensing: A Review. *ISPRS Journal of Photogrammetry and Remote Sensing*, **66**; 247–259

Nugroho, J. T., Zylshal, and D. Kushardono (2018). LAPAN-A3 Satellite Data Analysis for Land Cover Classification (Case Study: Toba Lake Area, North Sumatra). *International Journal of Remote Sensing and Earth Science*, **15**(1); 71–80

Ottosen, T.-B., G. Petch, M. Hanson, and C. A. Skjøth (2020). Tree Cover Mapping Based on Sentinel-2 Images Demonstrate High Thematic Accuracy in Europe. *International Journal of Applied Earth Observation and Geoinformation*, **84**; 101947

Phiri, D., M. Simwanda, S. Salekin, V. R. Nyirenda, Y. Mu-

rayama, and M. Ranagalage (2020). Sentinel-2 Data for Land Cover/Use Mapping: A Review. *Remote sensing*, **12**(14); 2291

Plakman, V., T. Janssen, N. Brouwer, and S. Veraverbeke (2020). Mapping Species at an Individual-Tree Scale in a Temperate Forest Using Sentinel-2 Images, Airborne Laser Scanning Data, and Random Forest Classification. *Remote Sensing*, **12**(22); 1–25

Resti, Y., C. Irsan, J. F. Latif, I. Yani, and N. R. Dewi (2023). A Bootstrap-Aggregating in Random Forest Model for Classification of Corn Plant Diseases and Pests. *Science and Technology Indonesia*, **8**(2); 288–297

Setiawan, Y., L. B. Prasetyo, H. Pawitan, L. Liyantono, Syartinilia, A. K. Wijayanto, and P. R. Hakim (2018). Pemanfaatan Fusi Data Satelit LAPAN-A3/IPB dan Landsat 8 untuk Monitoring Lahan Sawah. *Jurnal Pengelolaan Sumberdaya Alam dan Lingkungan (Journal of Natural Resources and Environmental Management)*, **8**(1); 67–76. (in Indonesia)

Sheykhmousa, M., M. Mahdianpari, H. Ghanbari, F. Mohammadimanesh, P. Ghamisi, and S. Homayouni (2020). Support Vector Machine Versus Random Forest for Remote Sensing Image Classification: A Meta-Analysis and Systematic Review. *IEEE Journal of Selected Topics in Applied Earth Observations and Remote Sensing*, **13**; 6308–6325

Shofiana, D. A., M. Caniadi, R. Sholehurrohman, and Aristoteles (2025). Decision Tree Algorithms in Water Quality Classification: A Comparative Study of Random Forest, XGBoost, and C5.0. *Science and Technology Indonesia*, **10**(4); 999–1011

Thanh Noi, P. and M. Kappas (2017). Comparison of Random Forest, K-Nearest Neighbor, and Support Vector Machine Classifiers for Land Cover Classification Using Sentinel-2 Imagery. *Sensors*, **18**(1); 18

Zhang, C., Y. Liu, and N. Tie (2023). Forest Land Resource Information Acquisition with Sentinel-2 Image Utilizing Support Vector Machine, K-Nearest Neighbor, Random Forest, Decision Trees and Multi-Layer Perceptron. *Forests*, **14**(2); 254

Zylshal, Zylshal, R. Wirawan, and D. Kushardono (2018). Assessing the Potential of LAPAN-A3 Data for Landuse/Landcover Mapping. *Indonesian Journal of Geography*, **50**(2); 184–196

Zylshal, Z., N. Sari, J. Nugroho, and D. Kushardono (2017). Comparison of Spectral Characteristic Between LAPAN-A3 and Sentinel-2A. In *IOP Conference Series: Earth and Environmental Science*, volume 98. IOP Publishing, page 012051

